

Few particle systems. An analysis of some strongly correlated states

N. Barberán¹ and J. Taron^{1,2}

¹*Departament de Física Quàntica i Astrofísica, Facultat de Física, Universitat de Barcelona, E-08028 Barcelona, Spain*

²*Institut de Ciències del Cosmos, E-08028 Barcelona, Spain*

(Dated: October 12, 2016)

The analysis of the quantum Hall response of a small system of ultracold bosonic atoms through the variation of its Hall resistivity against the applied gauge magnetic field, provides a powerful method to unmask its strongly correlated states in a quite exhaustive way. Within a fixed range of values of the magnetic field in the lowest Landau level regime, where the resistivity displays two successive plateaux, we identify the implied states as the Pfaffian and the state with filling factor $\nu = 2/3$.

PACS numbers: 03.75.Hh, 03.75.Kk, 67.40.Vs

I. INTRODUCTION

One of the main goals during a long time, related to many-body interacting systems, has been the localization and description of their stable states. A special role in the research effort is played by the strongly correlated states of charges under large magnetic fields [1, 2]. For some of these states, the analytical functions are available as in the case of the Laughlin [3] and the Pfaffian [4, 5] expressions. The Laughlin is the exact solution of a system under 2-body contact interaction and the Pfaffian is the exact solution for charges under 3-body contact interaction [6]. However, in general, the difficulty of the analysis has induced the development of the quantum simulation as one of the most fruitful ways to deal with the problem [7–9]. In the quantum simulation, charges are replaced by neutral cold atoms and real fields by artificial gauge fields.

Within the framework of quantum simulation, we analyze some features of relevant states. Our ansatz uses ultracold bosonic atoms and the artificial magnetic gauge field is associated with rotation of a parabolic potential that traps the bosonic cloud. We describe the system from the rotating frame of reference and employ the exact diagonalization technique.

The quantum Hall resistivity ρ_{yx} is used as a tool to show the presence of special (probably the most important) correlated states present at particular values of Ω , the frequency of the rotation that plays the role of an effective magnetic field. At those values of Ω the resistivity displays a plateau. We prove that the presence of impurities is crucial for its appearance and make a microscopic analysis of the process. To mimic an electric field, we consider a periodic perturbation along the X direction and study the time evolution of the generated current to model the transport equation and identify the resistivity. We concentrate on the case when Ω is strong enough to produce vortex-liquid states in the lowest Landau level (LLL) regime.

Some previous articles [10] that intended to classify the correlated states along the variation of the magnetic field, obtained the critical frequency (Ω_c) that marks a phase transition. There appear two phases: On the one hand the phase related to the Abrikosov vortex lattice states at large values of the filling factor (ν) or low values of Ω . On the other hand, the phase of vortex liquid states of low ν and strong magnetic

field. They obtained an estimated value of $\nu = 6$. However, all this analysis refers to a particular definition of the filling factor given by $\nu = \frac{N}{N_v}$ where N is the number of particles and N_v the number of vortices. They perform the calculation in a toroidal geometry that represents the bulk of a system containing a large number of vortices. Their conclusion was that "experiments access the quantum-melted vortex liquid phase will require specific attention to small system sizes and high angular momentum" for which, indeed, cases like the Laughlin or the Pfaffian type states preserve its full meaning.

Closely following our previous work [11] for $N = 4$ we focus on the Laughlin state and analyze the origin of the plateau of ρ_{yx} in the region where the expected value of the ground state (GS) angular momentum lies around 12 (in the circular symmetric case, $L_{GS} = N(N - 1)$ for the Laughlin state). Next we extend our analysis to $N = 5$. In this case, a huge time consuming effort would be required to obtain a Laughlin type state (at around $L_{GS} = 20$). However, despite the effort, the expectations of finding new physics beyond what was obtained already for $N = 4$ are very low. Aside from that, the presence of two pseudo-plateaux at lower values of Ω brings the opportunity to identify the associated states using different tools. E.g., the overlap with different analytical expressions or the analysis of the edge excitations. We found that the first plateau is related to the Pfaffian [4] state and the second one is well identified with the state of filling factor $\nu = 2/3$. The great interest on the Pfaffian is justified by the unique properties of its excitations [12, 13] that make it attractive in the context of topological quantum computation.

One of our main result is related to the fact that the analysis of the Hall response of the system provides, in an exhaustive way, the presence of all the correlated states that manifest themselves as plateaux of the resistivity.

The other main results is the direct observation of the ordered pattern of the GS, generated by 3-body contact interaction in the density. This allows us to give a nice interpretation of the Pfaffian state. Usually, the spatial correlation of the atoms is hidden in a circular symmetric state and the analysis of the two-body pair correlation function is necessary to uncover it. One atom is fixed at a given position \vec{r}_0 and the probability of finding the other ones around it, depends on this election. The existence of an impurity plays a similar role, the position of the impurity breaks the circular symmetry and the

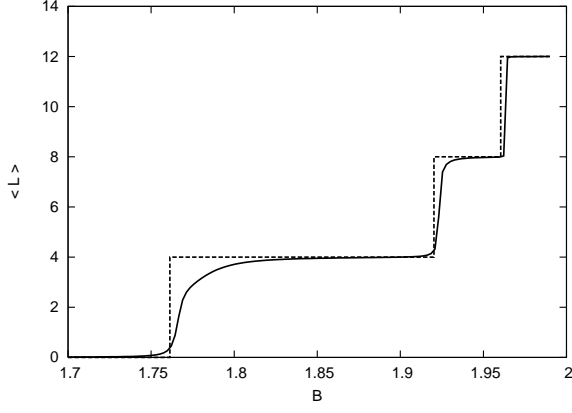


FIG. 1: Variation of the expected value of the angular momentum as a function of the magnetic field B . We consider $N = 4$, $Ng_2 = 6$, $\gamma = 0.1$ and $\mathbf{a} = (1, 0)$. The step-wise line refers to the symmetric case ($\gamma = 0$).

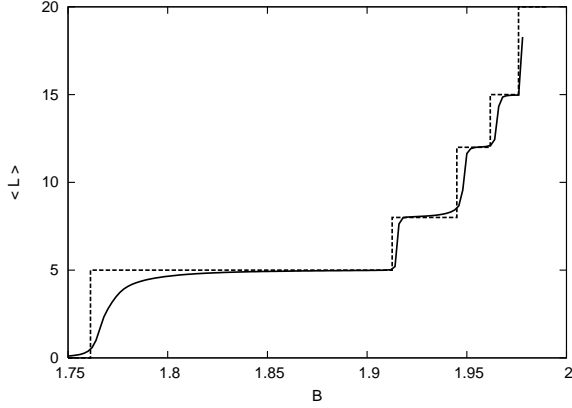


FIG. 2: The same as Fig. 1. for $N = 5$.

ordered pattern is explicit already in the density.

Our paper is organized as follows: In Section II we present our model, and a brief background of previous calculations on the Hall resistivity. An extra term for 3-body contact interaction is included. In Section III we analyze the origin of the plateaux that emerge in the resistivity at particular values of the magnetic field. We also study the transitions of the expected value of the angular momentum as the magnetic field increases and relate these transitions to the parity symmetry-breaking at the single-particle (sp) level. In Section IV we analyze the topological order related to the edge excitations. In Section V we show the numerical results and discuss their interpretation. Finally in Section VI we present our conclusions.

II. MODEL

We consider a system of N one-component bosonic atoms of mass M confined on the XY -plane. The cloud is trapped

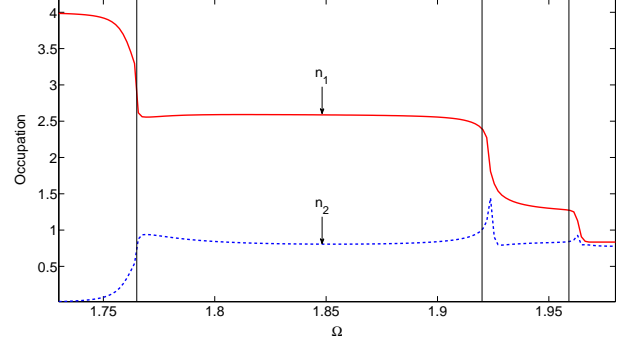


FIG. 3: We show the occupations of the first two orbitals as a function of $\Omega (= B)$. There is a correlation between the structure of the occupations and the jumps of $\langle L \rangle$ in a nearly symmetric system. For $N = 4$ the magic numbers of L in the symmetric case are $0 - 4 - 8 - 12$. We consider $Ng_2 = 6$, and $\mathbf{a} = (1, 0)$. The vertical lines at 1.761 , 1.920 and 1.960 mark the position of the jumps of L for the symmetric case.

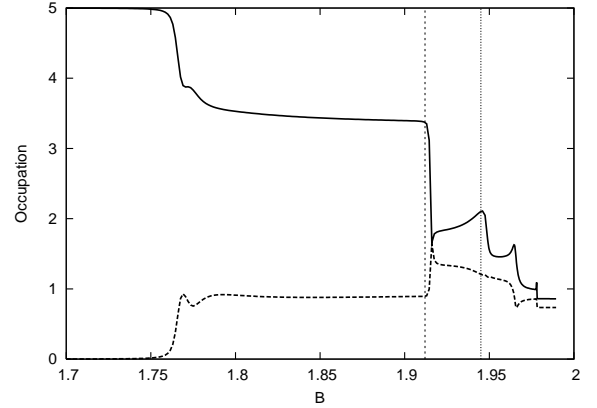


FIG. 4: The same as Fig. 3 for $N = 5$. The magic numbers of L in the symmetric case are $0 - 5 - 8 - 12 - 15$ and 20 . The vertical lines at 1.912 and 1.945 mark the positions of the jumps of L in the symmetric case, from 5 to 8 and from 8 to 12 respectively. We consider $Ng_2 = 6$, $\gamma = 0.1$ and $\mathbf{a} = (0.6, 0)$.

by a rotating parabolic potential of frequency ω_{\perp} and rotation Ω along the Z -axis. In the rotating reference frame the basic Hamiltonian (not including the perturbation along the X -axis) reads

$$\hat{H}_0 = \hat{H}_{sp} + \hat{H}_{int}, \quad (1)$$

where the single-particle (sp) part is given by

$$\begin{aligned} \hat{H}_{sp} = & \sum_{i=1}^N \left[\frac{1}{2M} (\hat{\mathbf{p}} + \hat{\mathbf{A}})^2 + \frac{1}{2} M \left(\omega_{\perp}^2 - \frac{(B^*)^2}{4M^2} \right) \hat{\mathbf{r}}^2 \right. \\ & \left. - \gamma \frac{\hbar^2}{M} \delta^{(2)}(\hat{\mathbf{r}} - \mathbf{a}) \right]_i, \end{aligned} \quad (2)$$

with

$$\hat{A}_x = \frac{B^*}{2} \hat{y}, \quad \hat{A}_y = -\frac{B^*}{2} \hat{x}. \quad (3)$$

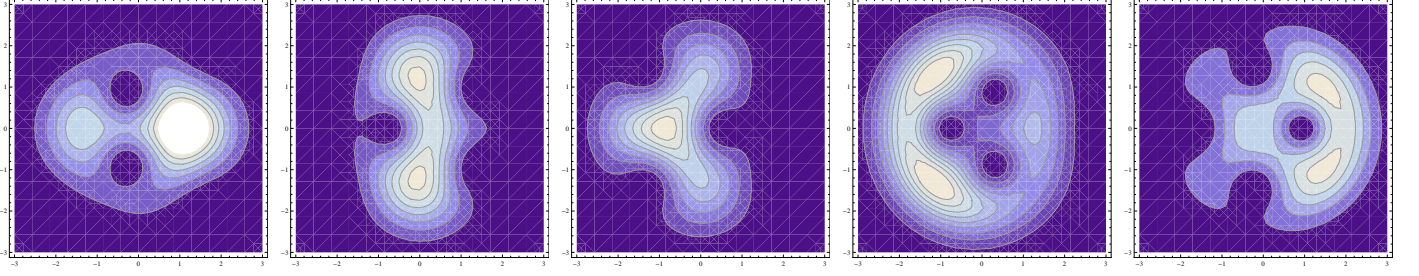


FIG. 5: Contour-plot of the density of the first five natural orbitals, the only ones with non-negligible occupations. The first one is localized at $\mathbf{a} = (0.6, 0)$. We consider $N = 4$, $Ng_2 = 6$, $\gamma = 0.1$, and $B = 1.963$.

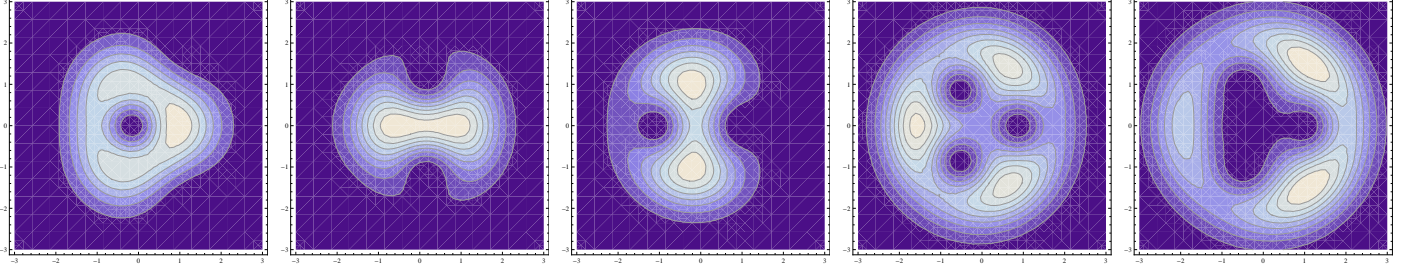


FIG. 6: The same as Fig.5 for $N = 5$. The first orbital is localized at $\mathbf{a} = (0.8, 0)$. We consider $Ng_2 = 6$, $\gamma = 0.1$, $B = 1.911$ and $g_3 = 2$.

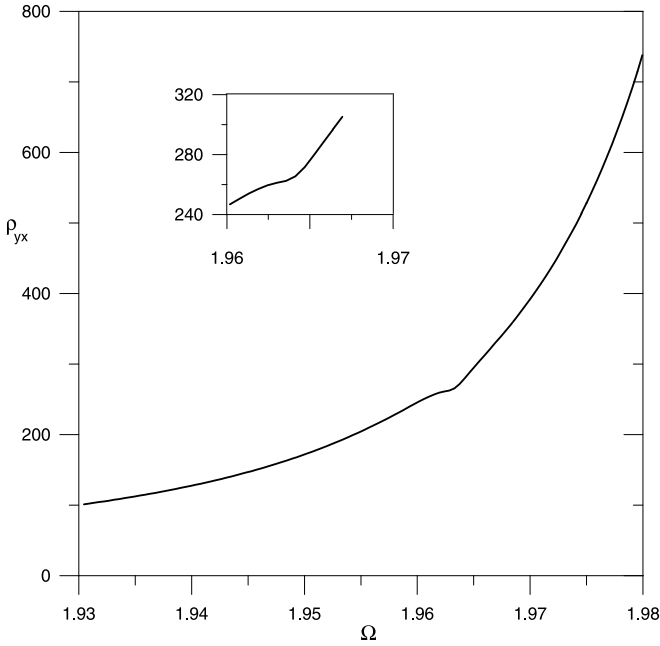


FIG. 7: Hall resistivity as a function of the magnetic field ($B = \Omega$) for $N = 4$ and $\mathbf{a} = (1.0, 0)$. The small plateau is approximately at $B = 1.963$.

The particular selection of the symmetric gauge has been done in the definition of $\hat{\mathbf{A}}$, with $B^* = 2M\Omega$ being the modulus of a constant artificial magnetic field directed downward along the Z -direction with $\mathbf{r} = (x, y)$. The last term in the sp Hamiltonian is due to the presence of an impurity modeled by

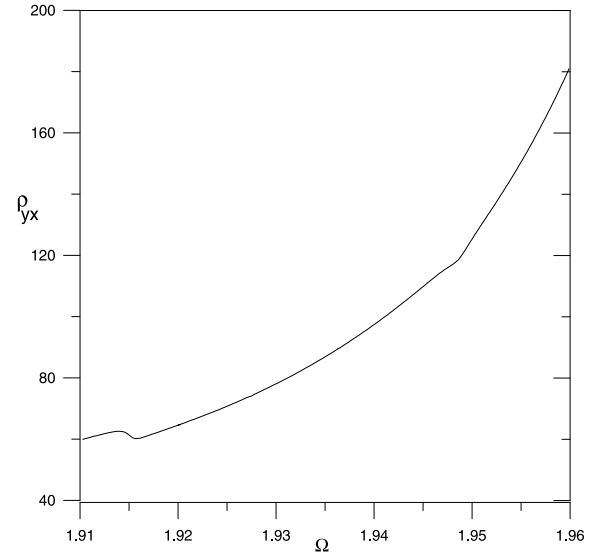


FIG. 8: The same as Fig.7 for $N = 5$, $\mathbf{a} = (0.6, 0)$, $\gamma = 0.1$ and $Ng_2 = 6$. The small plateaux are localized at approximately $B = 1.915$ and $B = 1.947$, no 3-doby interaction is consider.

a Dirac delta function. The dimensionless parameter γ measures its strength and \mathbf{a} localizes it on the XY plane. This term breaks the circular symmetry except for the case of an impurity localized at the center.

We model the atomic interaction by a 2D contact potential given by,

$$\begin{aligned}\hat{H}_{\text{int}} &= \frac{\hbar^2}{M} g_2 \sum_{i < j} \delta^{(2)}(\hat{\mathbf{r}}_i - \hat{\mathbf{r}}_j) \\ &+ \frac{\hbar^2}{M} \lambda_{\perp}^2 g_3 \sum_{i < j < k} \delta^{(2)}(\hat{\mathbf{r}}_i - \hat{\mathbf{r}}_j) \delta^{(2)}(\hat{\mathbf{r}}_i - \hat{\mathbf{r}}_k),\end{aligned}\quad (4)$$

where g_2 and g_3 are the dimensionless coupling parameters that give the strength of the 2 and 3-body interactions respectively and $\lambda_{\perp}^2 = \frac{\hbar}{M\omega_{\perp}}$.

In the LLL regime without impurities, the kinetic part of the Hamiltonian reads,

$$\hat{H}_{\text{kin}} = \hbar(\omega_{\perp} - \Omega) \hat{L} + \hat{N} \hbar \omega_{\perp}. \quad (5)$$

The sp solutions with well defined angular momentum m are the Fock-Darwin (FD) functions [14], given by $\phi_m(\theta, r) = \frac{e^{im\theta}}{\sqrt{\pi m!}} e^{-r^2/2} r^m$ where we consider λ_{\perp} as the unit of length.

Once the basic Hamiltonian (Eq.1) is solved, we proceed to diagonalize the one-body density matrix given by,

$$\hat{\rho}^{(1)}(\mathbf{r}, \mathbf{r}') = \langle \hat{\Psi}^{\dagger}(\mathbf{r}) \hat{\Psi}(\mathbf{r}') \rangle, \quad (6)$$

where the expected value is calculated at the GS and $\hat{\Psi}(\mathbf{r})$ is the field operator. The eigenfunctions are the one-body natural orbitals ψ_i , linear combinations of the FD functions, i.e. $\psi_i = \sum_0^{m_{\text{max}}} p_m^i \phi_m$. The eigenvalues are their occupations n_i , $i = 1, \dots, i_{\text{max}}$. Notice that m is angular momentum while i is an index that labels the eigenstates, namely $i_{\text{max}} = m_{\text{max}} + 1$, m_{max} is varied until convergence of the results.

If one of the natural orbitals is localized at the impurity, then we are able to distinguish between two types of states: localized and extended, a crucial condition necessary to understand the mechanism that produces a plateau as will be explained in section III.

Next we model the oscillating electric field $E_x(t)$ by an extra time dependent term in the Hamiltonian,

$$\hat{H}(t) = \hat{H}_0 + \hat{H}_{\text{pert}}(t) \quad (7)$$

given by

$$\hat{H}_{\text{pert}}(t) = -\lambda \frac{\hbar^2}{M\lambda_{\perp}^3} \left(\sum_{i=1}^N \hat{x}_i \right) \xi(t) \sin(\omega t) \equiv \sum_{i=1}^N E_x(t) \hat{x}_i \quad (8)$$

where λ is the dimensionless parameter that gives the intensity of the perturbation which we assume small. The explicit form of $\xi(t)$ is

$$\xi(t) = 1 - \exp[-(t/\sigma)^2], \quad (9)$$

where σ determines the velocity of the evolution of the induced density current.

The perturbation is switched on at $t = 0$ and, as t increases, the stationary regime is achieved when the amplitude of the oscillations become constant. From now on we consider $M = 1/2$ and $\hbar = 1$ and choose $\lambda_{\perp} = \sqrt{\frac{\hbar}{M\omega_{\perp}}} = \sqrt{2/\omega_{\perp}}$, $\hbar\omega_{\perp}/2$ and $\omega_{\perp}/2$ as units of length, energy, and frequency, respectively. With our unit of length, $\omega_{\perp} = 2$. Namely, for a single particle and a single impurity, we have

$$\begin{aligned}\hat{H}_i &= (\hat{\mathbf{p}} + \hat{\mathbf{A}})_i^2 + (\omega_{\perp}^2 - \Omega^2)(\hat{\mathbf{x}}^2 + \hat{\mathbf{y}}^2)_i + E_x(t) \hat{x}_i \\ &+ 2\gamma \delta^{(2)}(\hat{\mathbf{r}}_i - \mathbf{a})\end{aligned}\quad (10)$$

The effective trapping potential can be re-written as an oscillating trap of frequency ω aside from a spatial independent term,

$$(\omega_{\perp}^2 - \Omega^2) \left[\left(\hat{\mathbf{x}} + \frac{E_x(t)}{2(\omega_{\perp}^2 - \Omega^2)} \right)^2 + \hat{\mathbf{y}}^2 \right]_i. \quad (11)$$

That is to say, the cloud of atoms is dynamically forced by an oscillating term, while the impurity remains attached to a fixed position.

Finally, to identify the Hall conductivity σ_{yx} from the transport equation,

$$j_y(t) = \sigma_{yx} E_x(t) \quad (12)$$

we need to analyze the time evolution of the expected value of the current operator, $\langle \Psi(t) | \hat{j}_y | \Psi(t) \rangle$ where

$$\begin{aligned}\hat{j}_y(\mathbf{r}) &= \frac{1}{2M} \{ \hat{\Psi}^{\dagger}(\mathbf{r}) [\hat{\mathbf{p}}_y + \hat{\mathbf{A}}_y(\mathbf{r})] \hat{\Psi}(\mathbf{r}) \\ &- [\hat{p}_y - \hat{A}_y(\mathbf{r})] \hat{\Psi}^{\dagger}(\mathbf{r}) \hat{\Psi}(\mathbf{r}) \}.\end{aligned}\quad (13)$$

until the stationary regime is reached. Notice that the unusual expression of the current is due to the non-commutativity of the field operators.

To obtain $\langle \Psi(t) | \hat{j}_y | \Psi(t) \rangle$ we solve the time dependent Schrödinger equation $i\partial_t \Psi(t) = \hat{H}(t) \Psi(t)$ with the time-dependent Hamiltonian given by Eq.7.

Once we obtain the transverse conductivity σ_{yx} , we recover the resistivity from

$$\rho_{yx} = - \frac{\sigma_{yx}}{|\sigma_{yx}|^2 + |\sigma_{xx}|^2}, \quad (14)$$

where σ_{xx} comes from $j_x = \sigma_{xx} E_x$.

III. ORIGIN OF PLATEAUX

In this section, we focus on the mechanism that generates plateaux of ρ_{yx} within the LLL regime, namely, we refer to the fractional quantum Hall (FQH) scenario.

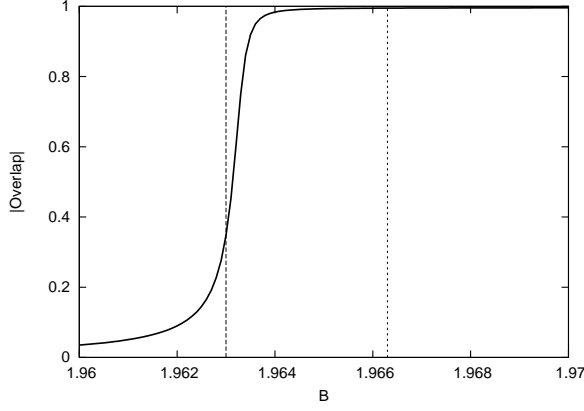


FIG. 9: Absolute value of the overlap between the exact solution and the analytical Laughlin expression as a function of B . $N = 4$, $Ng_2 = 6$, $\gamma = 0.1$ and $\mathbf{a} = (0.6, 0)$ is consider. Vertical lines mark the frontiers of B of the plateau, from $B = 1.963$ to 1.9663 .

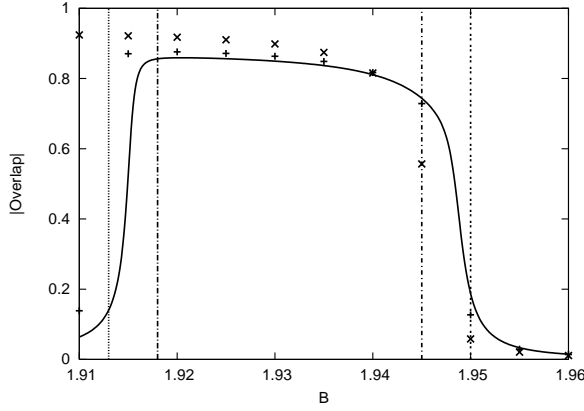


FIG. 10: The same as Fig.9 for $N = 5$. The analytical function considered on the overlap is the Pfaffian state. The significant values appear over the step $\langle L \rangle = 8$. The full line corresponds to $g_3 = 0$, the plus symbols to $g_3 = 1$ and the crosses to $g_3 = 5$. For all of them, $Ng_2 = 6$. We consider $\mathbf{a} = (0.6, 0)$ and $\gamma = 0.1$. The vertical lines mark the frontiers of the first (from 1.913 to 1.918) and the second plateau (from 1.945 to 1.95) respectively. Notice that in general, as the interaction grows, there is a shift to the left of the critical values of B where L jumps.

The plateaux we are interested on are labeled by a unique number, its filling factor, manifestation of the topological nature of the associated correlated states. In the interval between subsequent plateaux, the resistivity exhibits a linear behaviour given by

$$\rho_{yx} \sim \frac{B}{n_e} \quad (15)$$

reminiscent of the classical functionality [15]. n_e is the areal density of the extended part of the system, the part that contributes to the current \vec{j}_y . As B grows, the equivalent and simultaneous increase of n_e is necessary to maintain the resistivity constant. Then, during certain intervals of B transfer from localized to extended orbitals must take place, increasing

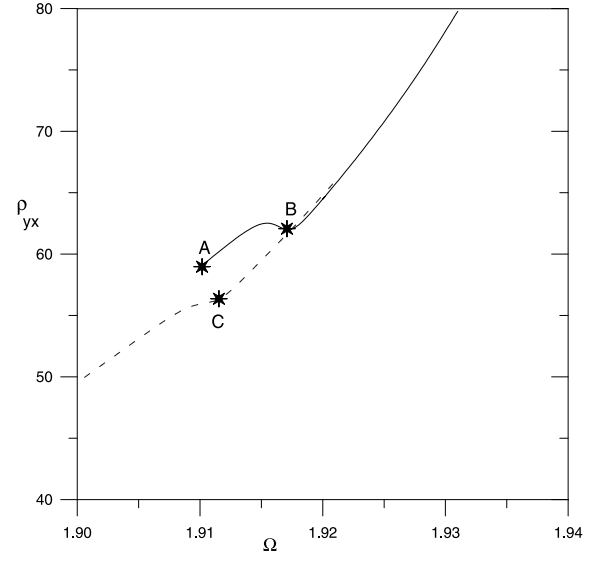


FIG. 11: Hall resistivity as a function of $B = \Omega$. The short full line contains only 2-body interaction ($Ng_2 = 6$), while the long one contains also 3-body interaction ($g_3 = 2$). We consider $N = 5$ and $\mathbf{a} = (0.8, 0)$. The marked points are: A (1.91, 58.94) and B (1.9172, 62.61) on the full line and C (1.911, 56.21) on the long dotted line.

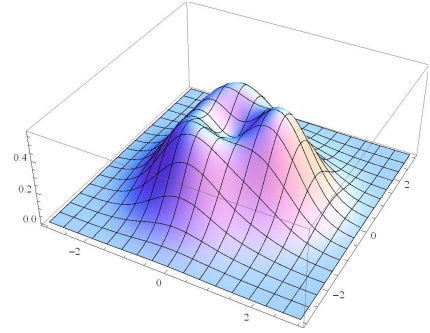


FIG. 12: 3D image of the GS density for $N = 5$ at $B = 1.911$ with an impurity at $\mathbf{a} = (0.8, 0)$ with $\gamma = 0.1$. We consider $Ng_2 = 6$ and $g_3 = 2$.

n_e . Impurities play the role of a reservoir of particles trapping or releasing them as B changes.

To be more precise, we analyze the properties of the GS. As B increases, the angular momentum of the system also increases. In the symmetric case (without impurities) where L is well defined, there are abrupt changes and only certain "magic" values of L are possible. For $N = 4$: $0 - 4 - 8$ and 12 and $0 - 5 - 8 - 12 - 15$ and 20 for $N = 5$. Differently, if some amount of asymmetry is included, the variation is soften and the expected value of the angular momentum has all the possibilities (see Figs.1 and 2).

On the other hand, if one looks at the occupations of the two most important natural orbitals (see Figs.3 and 4) one can verify that there is a correspondence between the angular momentum transitions and the significant variation of the occupations. The contribution of the FD states in the expansion of

the natural orbitals change as $\langle L \rangle$ changes as we will comment in the section of results.

Amazingly, in both analyzed cases, there is a clear localization at the impurity of one of the natural orbitals (see Figs.5 and 6). In both cases it is the first orbital with the largest occupation. Around the frontiers of the transitions, the decrease of n_1 means that transfer from localized to extended orbitals is possible and a plateau is expected. That is to say, intervals of B , where the occupations of the natural orbitals have a significant variation, turned out to be crucial to identify the regions where transfer is possible and plateaux are expected.

Fig.7 shows for $N = 4$ the appearance of a small plateau in the region where $\langle L \rangle$ changes from 8 to 12 and Fig.8 shows for $N = 5$ two pseudo-plateaux around the transitions from 5 to 8 and from 8 to 12 respectively.

It must be realized that these plateaux appear around special values of ρ_{yx} that localize states of significant interest, which would be characterized by fractional filling factors in the thermodynamic limit. Without impurities these values of ρ_{yx} would not be visible, due to the fact that the interval where n_1 decreases, would be reduced to a point and the plateau would disappear. Moreover, the extension of the plateau is related to the intensity of the impurity.

IV. EDGE EXCITATIONS

An extended way to identify the GS that results from exact calculations is by the overlap with a given analytical expression. However it has been stressed [16, 17] that a more convenient and non-ambiguous way is by its "topological order", a unique characteristic reflected in the properties of the edge excitations. This alternative becomes of special interest in our case, as in the calculation of the Hall resistivity all the spectrum is implied and not only the GS.

In the case of the Laughlin state for $N = 4$, this method provided the confirmation of its nature. We proved that the degeneracy of the edge excitations obey the theoretical predictions [18]: An excited state with $L = N(N - 1) + m$ is $p(m)$ times degenerated, where $p(m)$ are the partitions of m . It gives a sequence : 1 - 1 - 2 - 3 - 5 - 7 for $m = 0 - 1 - 2 - 3 - 4 - 5$. From our results, the plateau appears at about $\Omega/\omega_\perp = 0.982$ well inside the region where the expected value of the angular momentum is close to $L = 12$. To count out the number of excited edge states, we proceed as follows. We analyze the interaction energy (E_{int}) as a function of the angular momentum starting from $L = 12$. For each $L + m$ we obtain a column of eigenvalues. The distance between the lowest E_{int} and the next one at $L = 12$ defines a gap. In general, the number of values on the column $L + m$ that lies inside the gap, gives the number of the edge excitations for m . In particular, for the Laughlin state, all of them are degenerated. We obtain for $N = 4$ the sequence: 1 - 1 - 2 and for $N = 5$: 1 - 1 - 2 - 3 - 5 - 6.

It must be realized that the assignation of a filling factor of $\nu = 1/2$ to this state is due to the fact that the trapping potential is nearly suppressed by the strong rotation (see Eqs. 5 and 10), we end up with a nearly homogeneous system, for

which the filling factor is well defined (it does not depend on r). However, for other correlated states produced at lower values of the magnetic field, strong size effects prevent the association of a fractional filling factor, and the only justified assertion is that this state presents good symptoms to be identify with the correlated state with well defined filling factor in the thermodynamic limit. This is our case related to the states at the plateaux for $N = 5$ (see Fig.8).

The second plateau for $N = 5$ at $\Omega = 1.947$ (see Fig.8) has several properties that led us to the conclusion that it is the precursor of the correlated state with $\nu = 2/3$, well approximated by the composite-fermion (CF) model. The starting requirement is the identification of the angular momentum. This plateau lies within the region close to the angular momentum $L = 12$, one of the magic values for $N = 5$, related to incompressible states: the interaction energy does not change when the angular momentum is increased, the internal energy remains the same and the increase of the kinetic energy is due to the global movement of the center of mass. Once N and L are fixed, then as in the previous case, we proceed to count out the number of excited edge states.

Within the CF theory, the bosonic atoms are replaced by non-interacting composite particles consisting of a particle with a quantum of magnetic flux attached. These composite particles with fermionic statistics fill several LL in a compact way. At the end, the fractional filling factor for bosons is transformed into integer filling factor for the composite particles and the relation between the angular momenta is given by $L = L_{CF} + \frac{N(N-1)}{2}$ [18]. In our case it gives $L_{CF} = 2$ which has only one possible way to fill the Landau levels: 3 CF on the LLL and 2 on the first LL, this state is denoted as $\{3, 2\}$. Similarly, for $N = 6$, $L = 20$ and $N = 7$, $L = 30$ we obtain the CF states $\{4, 2\}$ and $\{5, 2\}$ respectively (in general $\{N - 2, 2\}$). For these three cases, the number of excited states evolves as: $N = 5$: 1 - 2 - 4 - 7, $N = 6$: 1 - 2 - 5 - 8 and $N = 7$: 1 - 2 - 5 - 9 for $m = 0 - 1 - 2 - 3$. This state in the thermodynamic limit belong to the series $\nu_F = \frac{p}{2p+1}$ [19] the values at which fractional quantum Hall is realized, p is the number of occupied LL's. For $p = 2$ it gives $\nu_F = 2/5$ and from the relation $\frac{1}{\nu_F} = \frac{1}{\nu_B} + 1$ valid for homogeneous systems [20] the filling factor for the bosonic system is $\nu_B = 2/3$. In agreement with the identification previously obtained in [17].

In the case of the state related with the first plateau at $\Omega = 1.915$ (see Fig.8), although the overlap with the analytical expression of the Pfaffian state is excellent (see Fig.10), the analysis of the number of edge excitations is not conclusive.

V. RESULTS

Our main result concerns, as mentioned previously, to our certainty of the presence of a precise number of correlated states below Ω_{max} , fixed by computational limitations. Moreover, we know at which values of Ω we must look for them. For $N = 5$ and $\Omega_{max} = 1.95$ we know that there are only

two correlated states and in this case, we were able to identify them with high probability. However, for larger values of Ω beyond Ω_{max} , we can not exclude the possibility to find new plateaux not identifiable with states properly modeled using the CF approach.

Once we have been able to generate plateaux and learned about their origin, the next step concerns to the classification of the implied correlated states and analyze their properties. We exploit several tools. A powerful one is the overlap of the exact solution with known analytical expressions.

For the Laughlin case we have [3]

$$\Psi^{Lau}(\{z_i\}) = \prod_{i < j} (z_i - z_j)^2 e^{-\sum |z_i|^2/2} \quad (16)$$

where $z_i = x_i + y_i$. Or for the Pfaffian [21],

$$\begin{aligned} \Psi^{Pf}(\{z_i\}) = & S \prod_{i < j \in \tau_1} (z_i - z_j)^2 e^{-\sum |z_i|^2/2} \\ & \times \prod_{k < l \in \tau_2} (z_k - z_l)^2 e^{-\sum |z_k|^2/2} \end{aligned} \quad (17)$$

where τ_1 and τ_2 means a partition of N . S indicates that the wave function is symmetrized over all the possible distributions of the particles into the subsets τ_1 and τ_2 .

Fig.9 shows for $N = 4$ the modulus of the overlap, $|\langle \Psi_{analytic} | \Psi_{exact} \rangle|$ [22] between the Laughlin state and the exact solution as a function of B . Although the exact solution contains a small amount of anisotropy, the overlap is extremely good, close to one along all the interval with angular momentum $L = 12$. This result confirms that the implied correlated state is the Laughlin, but also tells us that the overlap is not enough to localize the plateau. The main reason is that in the overlap only the GS is implied, whereas in the resistivity all the eigenstates play a role. The excited states suffer, along the interval of $L = 12$, a redistribution as B changes producing changes in the resistivity. One must look for the interval of B where n_1 decreases as it happens approximately between $B = 1.963$ and 1.967 , see Fig.3.

Fig.10 shows similar results for $N = 5$. In this case, in the overlap, the analytic Pfaffian expression is used. The interval with significant values corresponds to $\langle L \rangle = 8$ (see Fig.2) which is the angular momentum of the Pfaffian state for $N = 5$. In general, $L = \frac{N(N-2)}{2}$ for even N and $L = \frac{(N-1)^2}{2}$ for odd N [17]. In the full line only 2-body interaction was considered ($Ng_2 = 6$ and $g_3 = 0$) whereas for the plus and cross symbols, we used $g_3 = 1$ and 5 respectively. Although the overlap clearly improves when 3-body interaction is included, some amount of 2-body component must also be considered. If only 3-body interaction is used, although the interaction energy E_{int} of the GS vanishes, meaning that it is the solution of the 3-body Hamiltonian, we find zero overlap with the analytic expression (Eq.17). Roncaglia *et al.* in Ref. [12] propose an attractive and original protocol to generate and stabilize the Pfaffian state in a bosonic system submitted

to a rotating trap. They obtain that the best way to follow the scheme is by the suppression of the 2-body interaction. We were not able to reproduce this result and conclude that for this small number of particles, some amount of 2-body interaction is necessary to have a significant number of particles within each subset of the partition of N .

In a previous work [23], it was proven that at the sp level parity-symmetry breaking takes place during the evolution of Ω where the nucleation of the first vortex happens, namely close to the jump from $L = 0$ to $L = N$ (at about $\Omega = 1.76$ with our parameters). The most occupied natural orbital changes its sp momentum from $m = 0$ to $m = 1$. The use of the mean-field approximation (MFA) for low Ω is appropriate except within the narrow region where the vortex nucleation occurs. Differently, for large values of Ω where we cannot resort to the MFA, we find the following result: at the first plateau the most important component of ψ_1 (see Eq.6 and the paragraph below) changes from $m = 1$ to $m = 2$ whereas at the second plateau it changes from $m = 2$ to $m = 0$. We speculate with the possible relation between this behavior and the different shape of the plateaux (see Fig.8). However this interpretation requires deeper analysis.

Next, we perform a complete analysis of the density and pair correlation function at the three points marked in Fig.11. Only some special results are commented. We concentrate on the first plateau where the overlap with the Pfaffian state is the best. The selected points intend to give the following information: the point A (1.91, 58.94) not related to a plateau, is taken as a reference; the point B (1.9172, 62.61) on the plateau with only 2-body contact interaction and the point C (1.911, 56.21) with 2 and 3-body interactions.

We analyze in each case, the symmetric density ($\gamma = 0$) the density with the impurity and the function $\rho^{(2)}(\vec{r}_0, \vec{r})$. In all cases, the reference position \vec{r}_0 is the point where the symmetric density has its maximum.

At A we obtain the expected results for a non-correlated state. The symmetric density has a soft dimple at the center and exhibits a slight blown up at \vec{a} when the impurity is introduced, with otherwise no any sign of spatial correlation. The pair correlation function does not uncover any spatial order and at \vec{r}_0 the density is close to zero.

At B , the symmetric density is nearly flat with a slight maximum at the center. With the impurity, the density is blown up at \vec{a} and some subtle correlated positions appear around \vec{a} . The function $\rho^{(2)}$ exhibits an anomalous distribution, at \vec{r}_0 the density is significant. This point is a precursor of point C .

Finally point C shows an interesting result which drives us to give an interpretation of the meaning of the 3-body interaction. The symmetric density is quite flat with a slight minimum at the center, at odds with the point B . However, when the impurity is introduced, we obtain the density distribution shown in Fig.12. This figure provides some insight into the meaning of the 3-body interaction. Even though our system has $N = 5$, the density shows only three peaks. A possible explanation is as follows. The Pfaffian wave function is a symmetric combination of all possible partitions of N . For each

partition of N containing subsets τ_1 and τ_2 , in an effective way, the particles are classified : those in subset τ_1 and those in subset τ_2 . The repulsive 2-body interaction can only take place among particles pertaining to the same subset, let us call them i and j , and there is no interaction between particles in different subsets, let us call them i and k . Namely, i and k can exist at the same place, without feeling any interaction. This pair, however can interact with j at the same common place, realizing a 3-body interaction. The triangle shown in the figure is a consequence of this classification. If a particle in τ_1 is trapped at the impurity, only the other particles in τ_1 will accommodate far from it. The same happens for the particles in τ_2 trapped at the impurity which can survive with those in τ_1 . This mutual repulsion results in a triangular pattern shown in the figure.

VI. CONCLUSIONS

We have developed an effective way to find and eventually classify the correlated states of a cloud of cold bosonic atoms in the fractional quantum Hall regime.

We proved that although the overlap of the exact solution

with some analytical known expressions of the GS wave functions is a powerful way to identify the state, it does not provide any insight on the localization or extension of the plateaux of ρ_{yx}/B . The clue ingredient that localizes the plateaux is given by the behavior of the occupation of the natural orbital localized at the impurity.

The analysis of the GS density of the system that contains the impurity, gives the opportunity to learn about the meaning of the three body interaction, for a state close to the Pfaffian.

The properties of the edge excitations were used as a efficient tool to classify the state. Following the CF theory, we arrived to the conclusion that the second plateau is the precursor of a state of filling factor $\nu = 2/3$ in the thermodynamic limit.

VII. ACKNOWLEDGMENTS

We are indebted to Maciej Lewenstein for his important contribution. N.B. acknowledge partial financial support from the DGI (Spain) Grant No. FIS2013-41757-P. J.T. is supported by grants FIS2013-46570 and 2014-SGR-104.

-
- [1] E. Demler, Strongly correlated systems in atomic and condensed matter physics. Lecture notes for Physics 284. Harvard University (2011).
 - [2] M. Lewenstein, A. Sanpera, and V. Ahufinger, *Ultracold atoms in Optical Lattices: simulating quantum many body physics* (Oxford University Press, Oxford, 2002).
 - [3] R.B. Laughlin, Phys. Rev. Lett. **50**, 1395 (1983).
 - [4] G. Moore, and N. Read, Nucl. Phys. *B*360, 362 (1991).
 - [5] N. Read, Phys. Rev. *B*58, 16262 (1998).
 - [6] M. Greiter, X.G. Wen, and F. Wilczek, Phys. Rev. Lett. **66**, 3205 (1991).
 - [7] O. Boada, A. Celi, M. Lewenstein, and J.I. Latorre, Phys. Rev. Lett. **108**, 133001 (2011).
 - [8] J.I. Cirac, and P. Zoller, Nature Physics **8**, 264 (2012).
 - [9] I. Bloch, J. Dalibard, and S. Nascimbène, Nature Physics **8**, 267 (2012).
 - [10] N.R. Cooper, N.K. Wilkin, and J.M.F. Gunn, Phys. Rev. Lett. **87**, 120405 (2001).
 - [11] N. Barberán, D. Dagnino, M.A. Garcia-March, A. Trombettoni, J. Taron, and M. Lewenstein, New J. Phys. **17**, 125009 (2015).
 - [12] M. Roncaglia, M. Rizzi, and J.I. Cirac, Phys. Rev. Lett. **104**, 096803 (2010).
 - [13] B. Juliá-Díaz, T. Graß, N. Barbeán, and M. Lewenstein, New J. Phys. **14**, 055003 (2012).
 - [14] L. Jacak, P. Hawrylak, and A. Wojs, *Quantum Dots* (Springer Verlag, Berlin, 1997).
 - [15] D. Yoshioka, *The quantum Hall effect* (Springer Verlag, Berlin, 2001).
 - [16] X.-G. Wen, Adv. Phys. **44**, 405 (1995).
 - [17] M. A. Cazalilla, N. Barberán, and N. R. Cooper, Phys. Rev. *B*71, 121303(R) (2005).
 - [18] N.R. Cooper, and N.K. Wilkin, Phys. Rev. **B60**, 16279R (1999).
 - [19] B.I. Halperin, P.A. Lee, and N. Read, Phys. Rev. **B47**, 7312 (1993).
 - [20] X.C. Xie, S. He, and S. Das Sarma, Phys. Rev. Lett. **66**, 398 (1991).
 - [21] N.K. Wilkin, and J.M.F. Gunn, Phys. Rev. Lett. **84**, 6 (2000).
 - [22] B. Juliá-Díaz, and T. Graß, Comput. Phys. Commun. **183**, 737 (2012).
 - [23] D. Dagnino, N. Barberán, M. Lewenstein, and J. Dalibard, Nature Phys. **5**, 431 (2009).